OPTIMIZATION OF LITHIUM IRON PHOSPHATE BATTERY CHARGING AND PERFORMANCE

A. Misic

MITSG 14-12

Sea Grant College Program
Massachusetts Institute of Technology
Cambridge, Massachusetts 02139

Award No. N00014-13-1-0398

Project No. 2013-RU-022-LEV

Technical Report

Optimization of Lithium Iron Phosphate Battery Charging and Performance

Aleksandar Misic

September 3, 2014

Abstract

The goal of this project is to efficiently and safely charge a 5kWh battery pack in 15 minutes. Since the project is still in progress, this report describes experiments on a 56Wh battery. Experiments were performed to investigate various charging algorithms (Section 5.2.3), temperature effects (Sections 5.1.1-5.1.3 and 5.2.2) and long term health of the battery pack (Section 5.2.4). An introduction describing the motivation for the project is given in Section 1. Section 2 gives a detailed description of the equipment used including: cells, data acquisition devices, software, sensors, power sources and temperature control. Calculations performed on the data using matlab are explained in Section 3. The methods for running experiments are described in Section 4. Section 5.1 gives the results for single cell experiments while Section 5.2 gives results for the battery pack. Some conclusions are drawn in Section 6. The report is followed by a few appendices which contain extra graphs.

Contents

List of Figures

1 Introduction

Autonomous Underwater Vehicles (AUVs) are limited in their operating time by their battery life. The current method to recharge involves surfacing the vehicle, so an effort is being made to optimize underwater charging. With the ability to charge and transfer data underwater, AUVs will only need to surface for mechanical repair. With the current state of the art technology, a full underwater recharge can take over an hour. The motivation for this project is to recharge the battery pack of an AUV in under 15 minutes.

To achieve the fastest charge times, Lithium Iron Phosphate (LiFe-PO_4) batteries were chosen. Cells of this chemistry are very robust and can handle very high charge rates (4C) [1]. Tests were conducted to verify that charging at high rates does not adversely affect the cells in terms of discharge time. Generic lithium polymer cells of the same capacity were also charged at high rates for comparison. These results are graphically shown in Figure 24 on page 26, Appendix A. We can see that the Lithium polymer cells discharge time is significantly reduced when charge current increases, whereas LiFe-PO_4 batteries are unaffected by higher charging rates.

After these results were confirmed, all measurements, unless otherwise noted, were conducted at a 10A charge rate. Measurements were taken of time, cell voltage, current and temperature. From these values, we also deduced charge and discharge times, accumulated charge and energy and cell capacity (depth of discharge).

Once the room temperature characteristics were determined, the cells were subjected to various temperatures during charge and discharge. Tests were performed at temperatures ranging from 5°C to 45°C in 10°C increments. The 5°C tests are very important for our applications because water temperatures can reach close to 0°C.

2 Equipment

2.1 Cells

The LiFe-PO_4 cells used were A123 ANR26650. Since the nominal capacity is 2.5Ah [1] and the maximum recommended fast charge rate is 4C [1], this means we can safely charge the cells at $4 \cdot 2.5 = 10$A. The maximum rated operating temperature is 55°C [1], so we limited the temperature tests to 45°C assuming about 10°C rise while charging.

2.2 Data Acquisition

2.2.1 Single Cell Measurement

To measure the voltage, current and temperature, the National Instruments USB-6008 was used. The device has four differential channels with a resolution of 13 bits over a 10V range (1mV resolution). The voltage drop across a 0.1Ω series sense resistor was used to measure the current flowing into and out of the cell. A schematic diagram of this setup is shown in Figure 25 on page 27, Appendix B.

2.2.2 Multi-Cell Measurement

To measure current and temperature, the National Instruments USB-6218 device was used. This is a similar device to the USB-6008, but has 15 bit resolution and 16 differential channels. Seven of these channels were used for temperature, one for current.

Because of limitations in the common mode specifications of the National Instruments device, a custom circuit board using Texas Instruments TPS2481 Power Monitor ICs was used for voltage measurement. These are I^2C devices with 13 bit resolution [2]. Voltages were tapped at each cell so channel 1 reads the voltage from the positive terminal of cell 1 to ground, channel 2 reads the voltage from the positive terminal of cell 2 to ground, and so on. The total pack voltage is read by channel 7. A schematic is shown in Figure 26 on page 28, Appendix B.

2.3 Temperature Sensor

To measure ambient and cell temperatures, seven LM35 sensors in the TO-92 package were used. These devices share a common power supply of +5V from the USB-6218 as shown in Figure 26 on page 28. The analog voltage output of the LM35 is linearly proportional to temperature (10mV/°C). These sensors were placed on the surface of the cell with thermal grease.

2.4 Software

The software to control the USB-6008 and USB-6218 was written in C++ using the National Instruments library DAQMxBase. The channels were set up to record voltages every second and write them to a file. The file also contains the time each sample was taken, measured using the system clock. An Atmega328 micro controller was used to handle communication between the data logging computer and the TPS2481 array. The data was then processed using Matlab.

2.5 Power Supply

The power supply used was the Instek SPS-3610. This is a 36V/10A power supply with constant current and constant voltage modes.

2.6 Temperature Control

Cell temperature during charge and discharge was controlled using a refrigerator for temperatures below room temperature, and an air flow oven for temperatures above. In both cases, the battery was left in the environment for about 1 hour (soaking period) prior to charge to allow for the cell to be uniformly heated or cooled. The controlled temperatures for single cell tests were 5°C, 10°C, 35°C and 45°C; 5°C and 40°C for multi-cell experiments. Room temperature tests (assumed to be 25°C) varied between 20°C and 27°C.

2.6.1 Air Flow Oven

To heat the cells, a VWR Symphony air flow oven was used. Two curves, shown in Figure 27 on page 29, Appendix C, are of the temperature of the oven and of the cell. We can see that the cell temperature lags behind the environment temperature during the soaking period.

2.6.2 Refrigerator

The refrigerator used was a 1.7 cubic foot refrigerator capable of temperature ranges from 4°C to 15°C. Its small size and limited capabilities for control lead to temperature fluctuations as shown in Figure 28 on page 30, Appendix C.

3 Calculations

3.1 Voltage, Current and Power

Calculations for all parameters were done in Matlab. Current as a function of time was calculated by $I_{cell}(t) = V_{shunt}(t)/0.1\Omega$, where $V_{shunt}(t)$ is the voltage drop across the sense resistor. Current flowing into the cell (charging) was defined as positive current, while discharging is represented by a negative current. The time varying power function was calculated as the product of cell voltage and current $P_{cell}(t) = V_{cell}(t) \cdot I_{cell}(t)$.

These calculations are the same for the multi-cell experiments except that voltage was measured using absolute references as shown in Figure 26 on page 28, Appendix B. To obtain individual cell voltages, the readings from each channel were subtracted from the next. The total pack voltage is the raw data from channel 7.

3.2 Charge and Discharge Times

Charge time was assumed to be the time while the cell current was above 9A, and discharge times were assumed to be the time while cell current was below -0.1A and voltage was above 3.2V.

3.3 Accumulated Energy and Charge

The energy function is given by: $E(t) = \int P(t)dt$, similarly, the charge function is given by: $q(t) = \int i(t)dt$. Accumulated energy and charge are the maximum values of the two functions, respectively. Note that $E(0) = q(0) = 0$ is the assumed initial condition even though there is still some charge left in the battery after the last discharge cycle.

The calculations for the multi-cell pack are the same. Since we have a power function for each cell independently, but only one current function (the current through all cells is the same and only measured at one point), we have energy curves for each cell, but only one charge curve for the battery pack.

3.4 Capacity

Cell capacity, or more accurately depth of discharge (DOD), was calculated as the sum of the product of instantaneous current and sampling period in seconds during the discharge phase. The result was divided by 3.6 to get values in units of mAh.

4 Procedure

4.1 Conditioning

One conditioning cycle is defined as charging the cell to 3.6V at 2A and discharged by a 5Ω resistor ($\sim$ 0.6A) down to 2V. Once 2V is reached, the load is changed to a 1KΩ resistor for approximately 45 minutes to stabilize the electrolytes. The voltage recovers slightly and the cell is ready for the next conditioning cycle. Three such cycles were performed to fully condition the cell. During the first cycle, charging voltages were irregular with many fluctuations. Also, the discharge stage of the first few conditioning runs are much longer than later cycles. This procedure is done to bring the cell to a known state before taking measurements. After two cycles, the voltages stabilize and become predictable. All cells placed in the pack were conditioned beforehand.

4.2 Charging

The cell was charged to 3.6V at a rate of 4C (10A) with a floating (not earth ground referenced) power supply. This charging algorithm is known as constant current (CC) and is the manufacturer recommended algorithm for fast charge. This same method was used for multi-cell charging with the cutoff condition being when the *average* of cell voltages is 3.6V.

4.3 Discharging

Once the cell was charged, the power supply was immediately shut off and the discharge phase was started. Discharging was done by a fixed 5Ω resistor, so the current varied slightly proportional to the cell voltage. The cut off voltage for discharge was 2V.

This procedure was also used for multi-cell discharging, except the load resistor was $7 \cdot 5\Omega = 35\Omega$ to keep the same discharge rate. Also, discharging was stopped when the pack voltage reached $7 \cdot 3.2V = 22.4V$. Initial trials showed that bringing the cells in the pack down to 2V creates a large unbalance and cells prematurely fail.

5 Results and Analysis

5.1 Single Cell

The initial tests were performed on a single cell to determine baseline temperature characteristics. The results would theoretically also apply to a battery pack of multiple cells. The following sections refer to tests performed on a single 3.3V nominal LiFe-PO_4 cell. For all experiments, the charging

algorithm was CC at 10A until the cell reached 3.6V. A photograph of the single cell setup is shown in Figure 1.

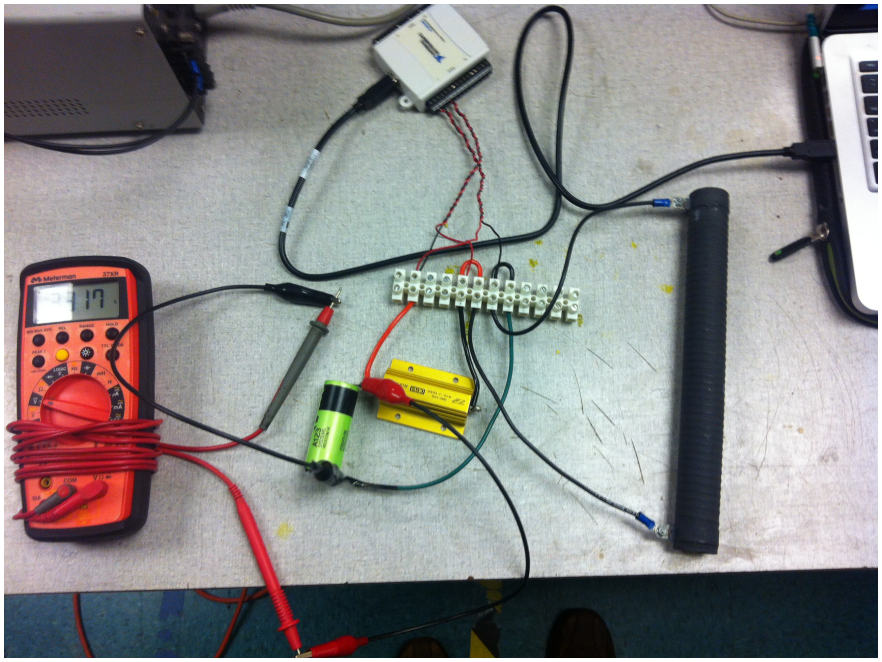

Figure 1: A photograph of the single cell measurement setup with a multi meter for control.

5.1.1 Room Temperature Tests

After each cycle at temperature, a room temperature cycle was performed to make sure the temperature did not affect the operation of the cell. From the graph in Figure 2 on the following page, we can see that the cells did not experience thermal shock. The line colors correspond to the cell temperature of the preceding cycle and are explained in the legend.

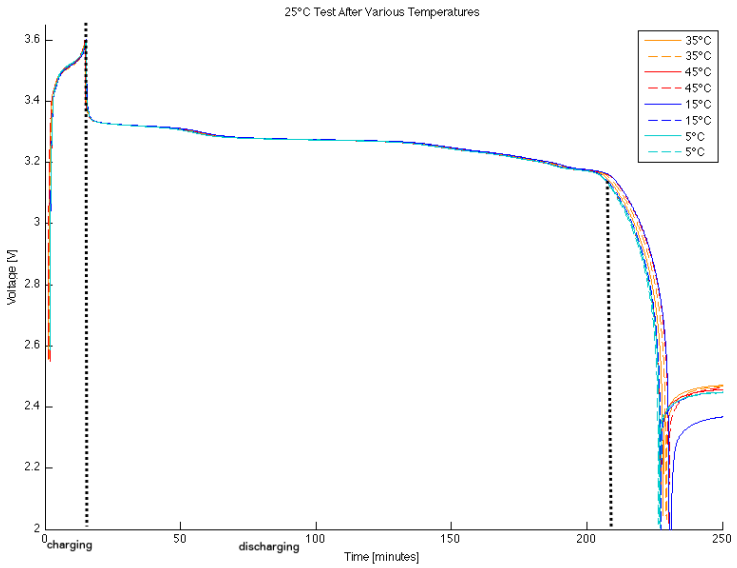

Figure 2: Charge and discharge curves of cycles conducted at room temperature. Variations are due to varying temperature of the laboratory. *Note: The first post-15°C run has a lower recovery voltage because the cell was discharged to 1.8V instead of 2V.*

5.1.2 Cooled Tests

To test the performance at temperatures below 25°C, the cells were cooled down to 5 and 15°C. We found that the time to charge decreased with lower temperatures, but so did the operating (discharge) time. This tells us that when charging at lower temperatures, energy is not efficiently transferred to the cell. Figure 3 on the next page shows a room temperature cycle and two cycles at lower temperatures. The initial few minutes of charging in the 5°C case overshoots the 3.6V limit, then the voltage drops slightly before coming to the final peak. This indicates that during the first few minutes, the cell is heating up to a reasonable temperature.

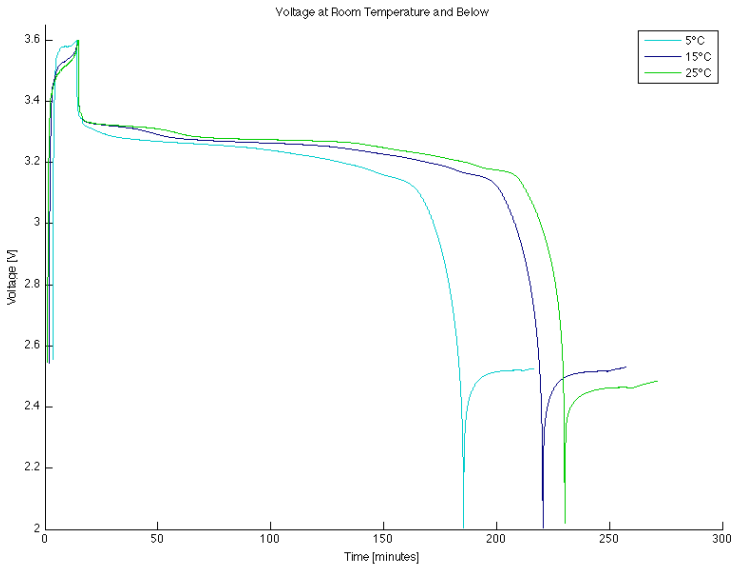

Figure 3: Charge and discharge curves of cycles conducted at room temperature and below. *Note: Curves were lined up to the beginning of discharge to give an accurate representation of differences in discharge time.*

5.1.3 Heated Tests

The cells were heated to 35°C and 45°C to test above room temperature conditions. The voltage curves are shown in Figure 4 on the following page. We can see that with increased temperature, the charge phase is longer in time, but this leads to a much longer operating time. The average voltage during the charging phase is lower. A zoomed in view of cold and hot runs is shown in Figure 5 on the next page. The complete dataset is given in Figure 29 on page 31, Appendix D.

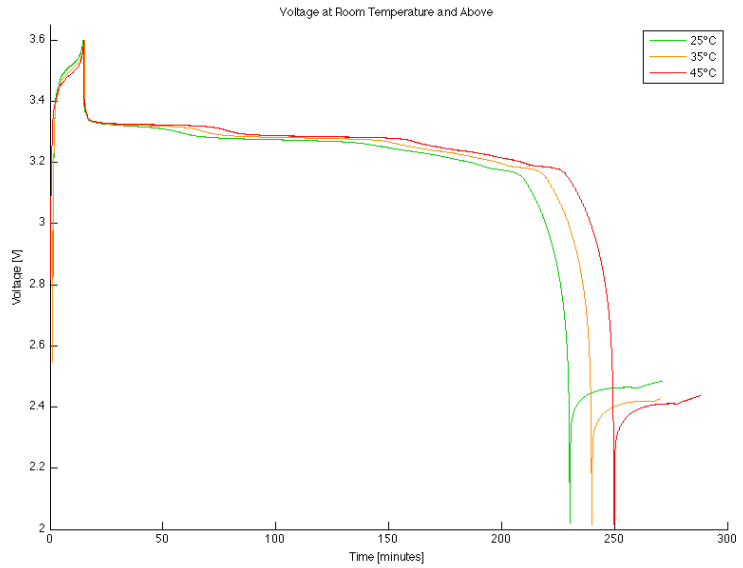

Figure 4: Charge and discharge curves cycles conducted at room temperature and above. *Note: Curves were lined up to the beginning of discharge to give an accurate representation of differences in discharge time.*

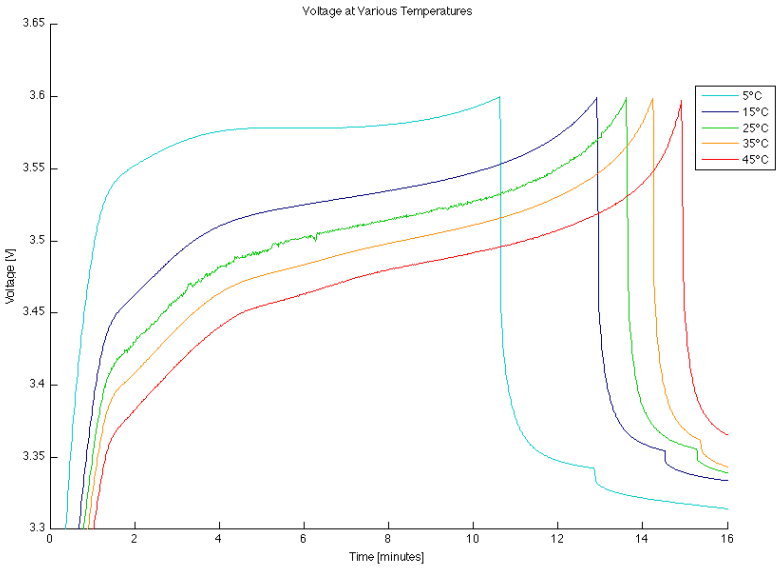

Figure 5: A zoomed view of the curves in Figures 2 and 3. *Note: the curves were shifted in time so that the beginning of the charge phase is set to 0 minutes. This clearly shows the change in charge time.*

5.1.4 Energy Analysis

The accumulated energy for each cycle is shown graphically in Figure 6. The hotter runs accumulate more energy compared to lower temperatures. We can also see that with increasing temperature, the final energy after discharge is lower than colder runs. This tells us that discharging at higher temperatures makes better use of the batteries stored energy.

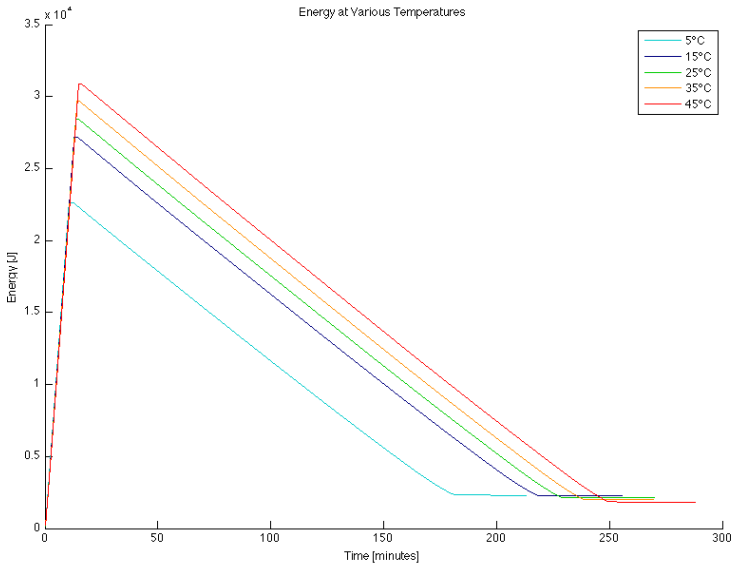

Figure 6: Plot of energy for all temperature cycles

5.1.5 Changing Temperature Tests

Another test which was performed was to charge the cell at one temperature and discharge at another. Figure 7 on the following page shows these results with constant temperature tests as well. We can see from the plots that changing temperatures only slightly affect the results, not enough to make a significant improvement or degradation to the discharge time.

5.1.6 Temperature Analysis

A plot of temperature rise is shown in Figure 8 on the next page. We can see that at low temperatures (5 to 25°C) the cell temperature rises about 10°C. For high temperatures, there is less of a temperature increase (approx. 5°C). This result tells us that more energy is used to heat the cells at lower temperatures, therefore, less electrical energy is delivered to the cell.

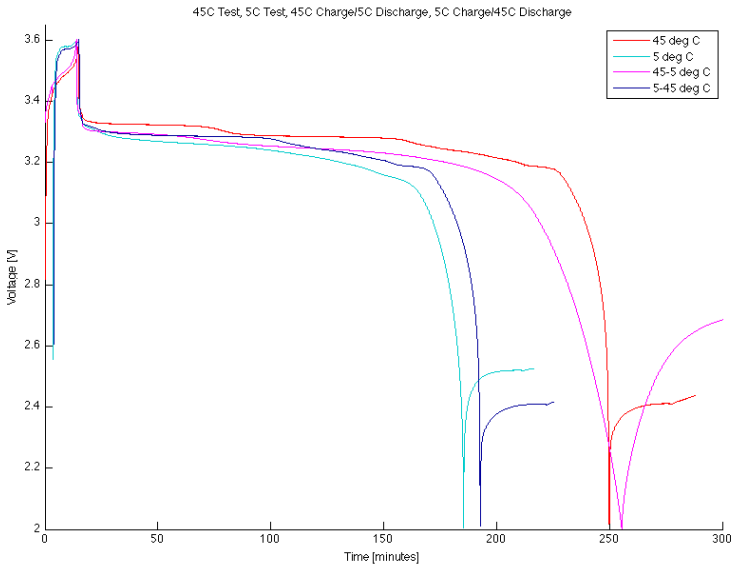

Figure 7: Plot of constant temperature cycles: 45°C (red) and 5°C (cyan) and varying temperature cycles: 45°C charge with 5°C discharge (magenta) and 5°C charge with 45°C discharge (blue).

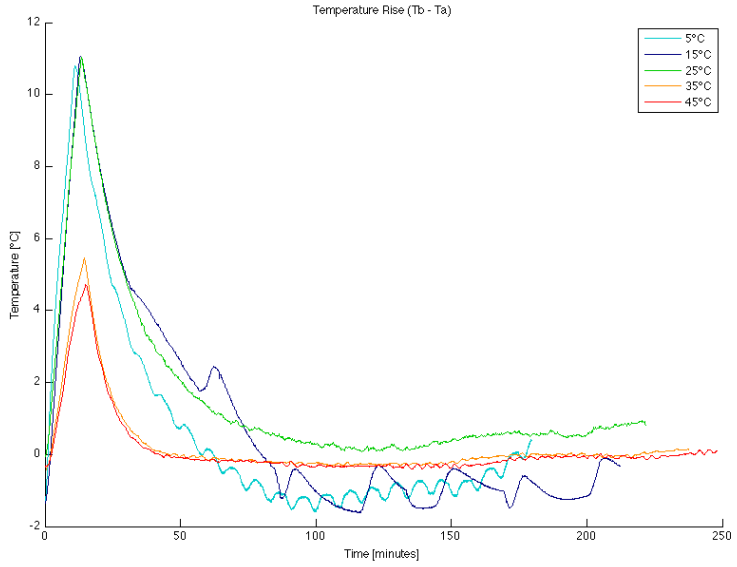

Figure 8: Plot of cell temperature rise. To clearly show all results, ambient temperatures (Ta) were subtracted from cell temperature (Tb).

5.1.7 Numerical Results

The results from the experiments are given numerically in Table 1 below. The percent difference from 25 °C is given in Table 2. Two parameters, E/t_{Charge} and $t_{Discharge}/t_{Charge}$ were also calculated and remain relatively constant throughout the experiment.

Mean values of parameters at given temperature					
Temperature [°C]	5	15	25	35	45
Charge Time [m:s]	10:25	12:50	13:21	14:07	14:46
Discharge Time [h:m]	2:48	3:25	3:31	3:43	3:53
Accumulated Energy [kJ]	22.428	27.278	28.198	29.585	30.862
Accumulated Charge [C]	6308.1	7787.4	8082.3	8531.1	8936.6
Capacity [mAh]	1750.7	2156.7	2236.7	2366.0	2478.4
$\frac{DischargeTime}{ChargeTime}$ [s/s]	16.08	15.96	15.87	15.82	15.78
$\frac{Energy}{ChargeTime}$ [W]	35.89	35.45	35.19	34.94	34.82

Table 1: Numerical results from temperature experiments (average of all cycles).

Percent difference of parameters from 25 °C				
Temperature [°C]	5	15	35	45
Charge Time [%]	-24.73	-4.06	5.51	10.07
Discharge Time [%]	-23.41	-3.50	5.18	9.52
Accumulated Energy [%]	-22.79	-3.32	4.80	9.02
Accumulated Charge [%]	-24.66	-3.72	5.40	10.04
Capacity [%]	-24.38	-3.64	5.62	10.25
$\frac{DischargeTime}{ChargeTime}$ [%]	1.34	0.56	-0.32	-0.55
$\frac{Energy}{ChargeTime}$ [%]	1.97	0.74	-0.71	-1.05

Table 2: The same data as table 1, but expressed as a percent difference from 25°C results.

The results from table 2 have been plotted in Figure 9 on the following page to give a clear visual interpretation of the results. We can see that there is a linear correlation between temperature and all parameters while the temperature is above 10°C. Below 10°C, the results drop drastically.

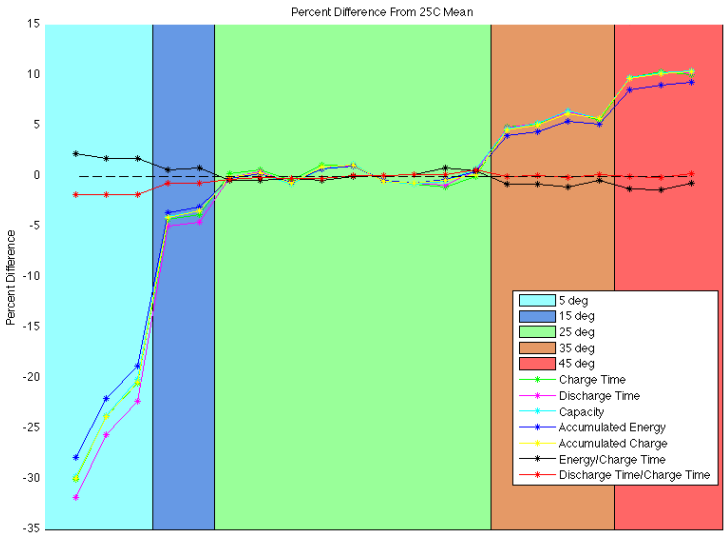

Figure 9: Graphical interpretation of results from Table 2. The background color depicts the temperature at which tests were conducted.

5.2 Multi-Cell

To give more meaningful results, a realistic battery pack of seven series connected cells was made. This provides a 25.2V maximum, 23.1V nominal total voltage. Unless otherwise stated, all tests were charged at 10A (CC). A photograph of the multi-cell setup is shown in Figure 10 on the next page.

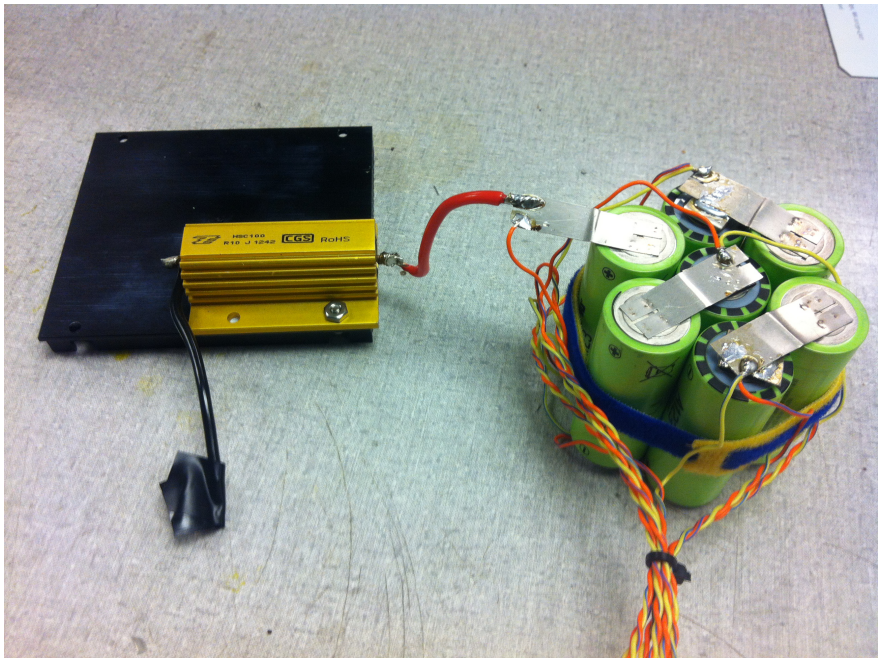

Figure 10: A photograph of the multi-cell measurement setup.

5.2.1 Cell Configuration

Another reason for the choice of seven cells, is that they can be conveniently packaged in a honey comb pattern. This is a common way to connect batteries in an AUV, and we also wanted to see the effects of temperature rise within the pack, i.e., how the innermost cell would be affected by the temperature rise of surrounding cells. A 3D model of the pack is shown in Figure 11.

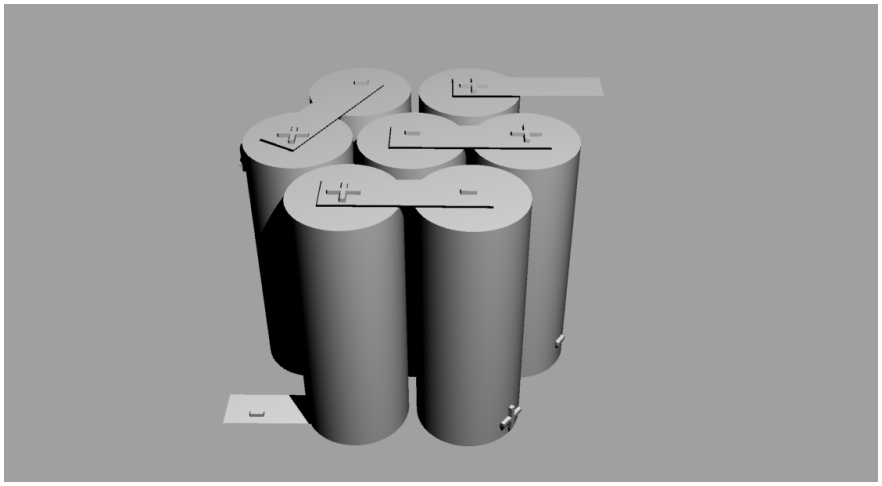

Figure 11: A 3D model of the battery pack with tabs showing the connections.

5.2.2 Temperature Tests

To compare with the single cell tests, the pack was subjected to ambient temperatures of 25°C, 5°C and 40°C. The hottest temperature attempted was 40°C because, after initial room temperature results, we expected approximately 15°C rise in the inner most cell. This would raise the temperature of the cell to the maximum allowable operating temperature specified by the manufacturer. Results from these experiments are shown in Figure 12.

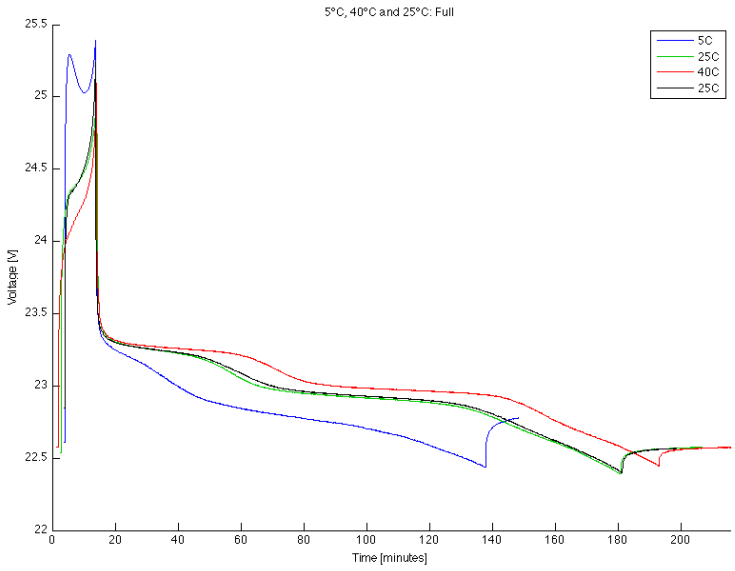

Figure 12: Plot of voltage for all temperature tests. The full pack voltage is plotted by taking the raw measurement from channel 7 of the TPS array.

Due to balancing issues during charging, the results are not as dramatic as in the single cell tests. Not all cells were charged to their full capacity, so the lowest voltage cell fell below the cut-off limit before the other cells and the experiment was terminated. Individual cell voltages are shown in Figures 31 to 33 on pages 33–35, Appendix E, clearly showing the balancing issue. This was noticed in the 25°C experiment, and the effect is more significant at higher temperatures.

5.2.3 Charging Algorithms

To overcome the balancing issue, different charging algorithms were used on the pack to see if the unbalance would decrease. Three algorithms were compared: CC, Constant Current/Constant Voltage (CC/CV), and an incremental decrease in current specified by charging time. The CC method is the same as described for previous tests. CC/CV is a 10A charge until the pack voltage reaches 25.2V, then the power supply is switched to constant voltage mode and the current drops until charging is complete. Incremental decrease in current is the same as the CC algorithm, but after 6 minutes, the current drops from 10A to 6A for 2 minutes, then down to 4A for 2 minutes and finally at 2A until the pack voltage reaches 25.2V. A plot of these current profiles is shown in Figure 13 on the following page. The voltage plots of the complete charge/discharge cycles are shown in Figure 14 on the next page. We can see that the discharge time is increased

with the different charging algorithms, but the individual cell voltages during charge (Figures 34 to 36 on pages 36–38, Appendix F) tell us that unbalance is actually worse with the different algorithms.

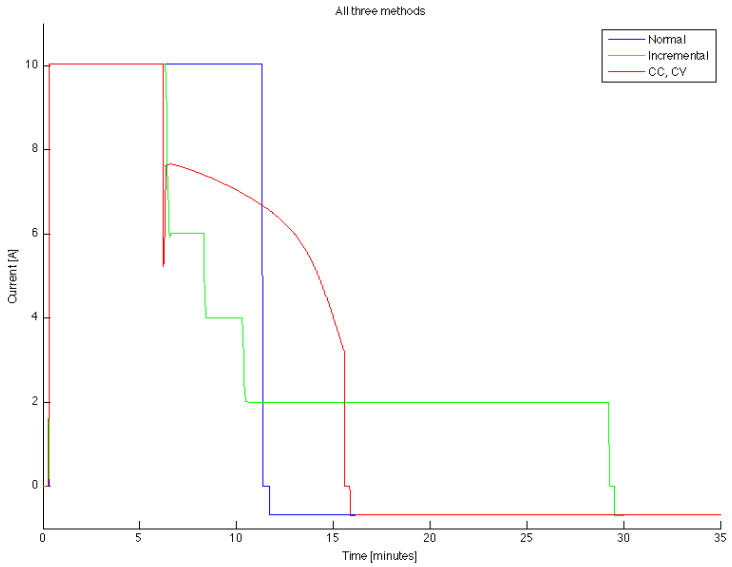

Figure 13: Plot of currents for CC (Normal), CC/CV and incremental algorithms.

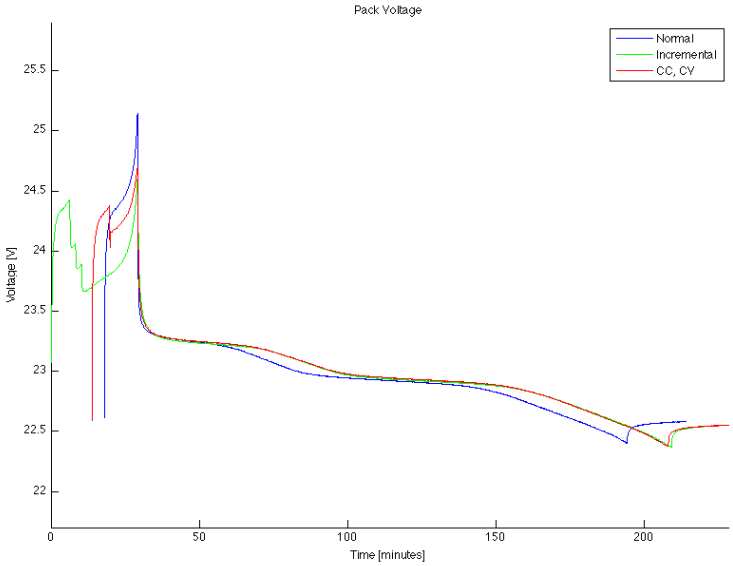

Figure 14: Plot of voltages for CC, CC/CV and incremental algorithms.

5.2.4 Life Tests

With each cycle, the pack becomes more and more unbalanced with the highest voltage cell (cell 7) increasing the most, and the lowest voltage cell (cell 1) not charging to its maximum potential. To investigate the problem, we set up an automated cycling station and ran full cycles until the minimum voltages became unacceptable. This occurred after about 50 cycles. At the beginning of the experiment, cells 7 and 1 were swapped to see if they would return to their respective positions after being part of an initially unbalanced pack. Figures 15 to 16 on pages 19–20 show the first and last charges of this experiment.

Figures 17 to 18 on pages 20–21 show the maximum and minimum voltages of all cycles of the life test. There was some loss of data for the last few samples in early cycles, so the voltages plotted do not correspond to the actual maximum or minimum voltage the pack experienced. The same applies for minimum voltages, but the error is less noticeable because the voltage changes less in the last few seconds of the discharge phase. Also, the first few cycles were not performed using the automated setup, so there is some variation due to human error.

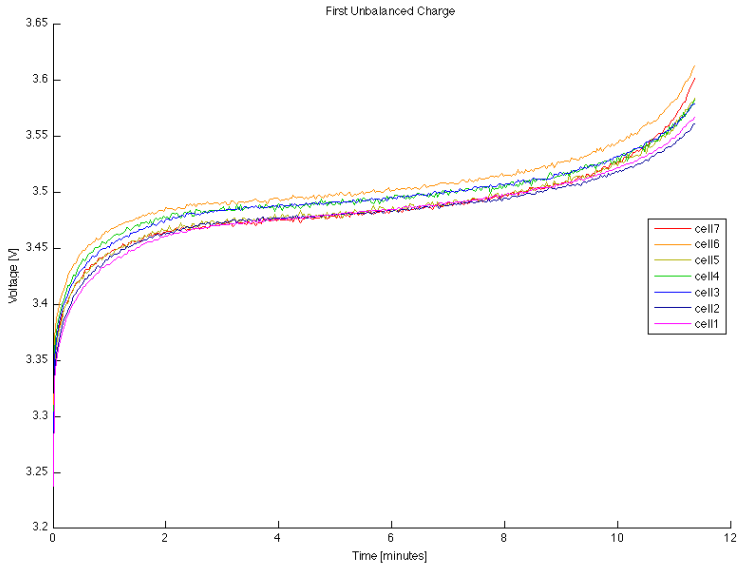

Figure 15: Charge curve of the first cycle in pack life test

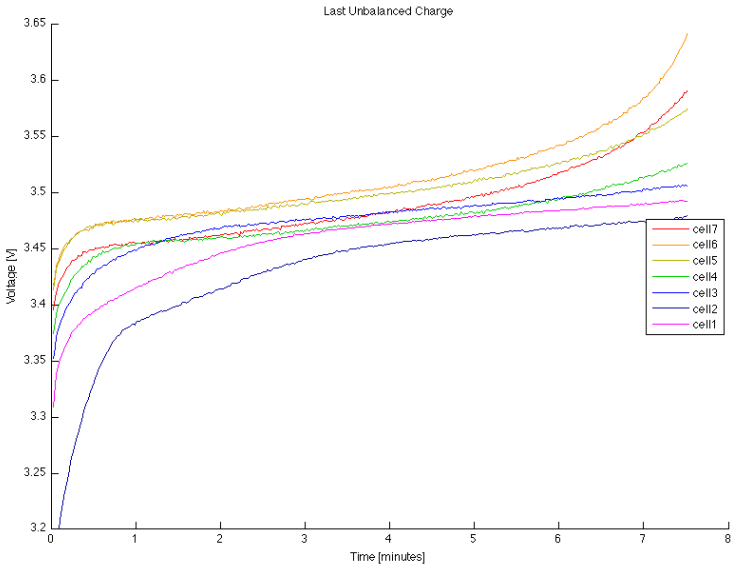

Figure 16: Charge curve of the last cycle in pack life test

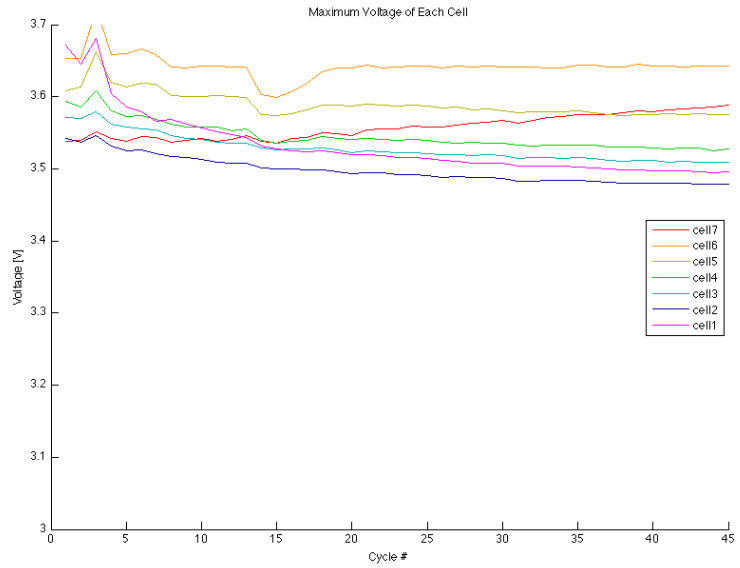

Figure 17: Plot of maximum voltages during charge phase vs. cycle number.

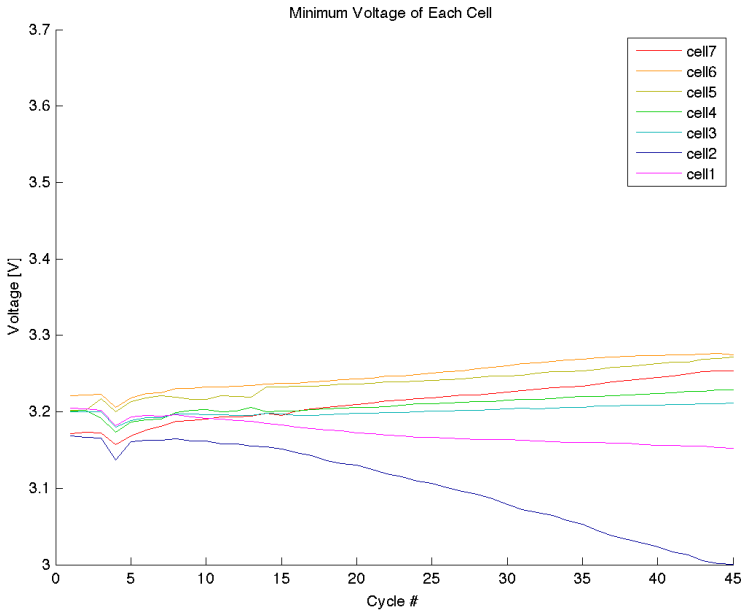

Figure 18: Plot of minimum voltages during discharge phase vs. cycle number.

5.2.5 Balancing

To properly balance the pack, an analog circuit was implemented and is schematically shown in Figure 19 on the following page. There are two parts to the circuit, a 9-36V to 15V DC/DC converter to power the comparator, and the balancing circuit itself. The idea behind this system is to divert current from the highest cell to lower cells once a voltage of 3.6V is detected. In other designs, power resistors are used to dissipate the power, but this is not practical inside an AUV due to size and heat. The circuit shown in Figure 19 on the next page is only one of the seven used to balance the pack.

The operation of the circuit is as follows: the isolated DC/DC converter takes power from the charging voltage source as an input and provides 15V above the respective cell's negative terminal to the comparator. The negative input takes a reference voltage of 3.6V (trimmed by the potentiometer) and the positive terminal is connected to the positive terminal of the cell. When the cell voltage reaches 3.6V, the comparator drives the MOSFET gate with about 6V to partially turn the MOSFET on allowing some current to bypass the cell. When this happens, the cell voltage drops below the cutoff point, and the comparator turns the MOSFET off. The cell starts charging again and exceeds 3.6V and the cycle repeats. This oscillation allows for the cell to effectively remain at 3.6V until lower voltage cells catch up to the 3.6V limit. The process is the same for each cell in the pack. Figure 20 on the following page is a screen capture from an oscilloscope measuring voltage and current on a single cell.

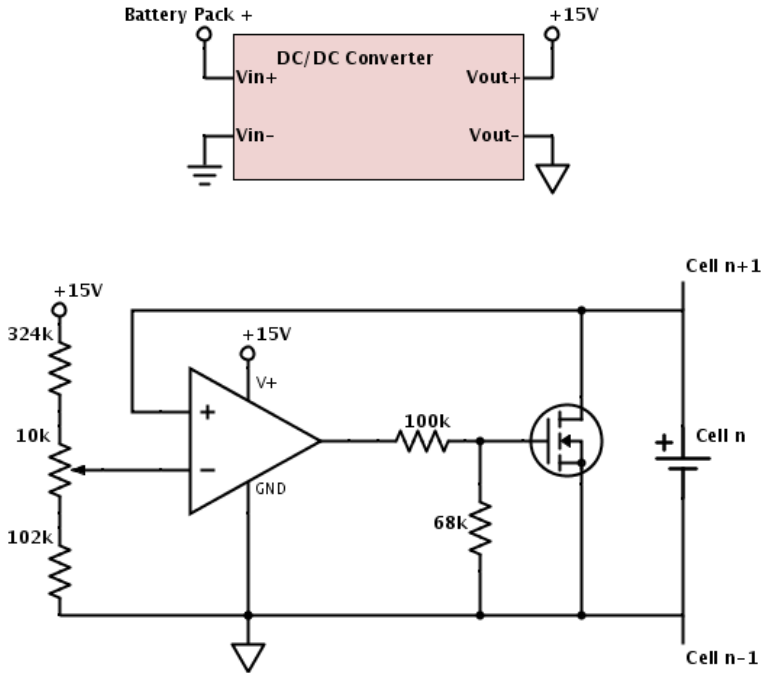

Figure 19: Schematic diagram of balancing circuit. These are the components used for any of n cells in the pack. It employs an isolated flyback DC/DC converter whose input is the pack voltage and is common to all n balancing circuits in the pack. The output ground is tied to the negative terminal of cell n (positive of cell n-1).

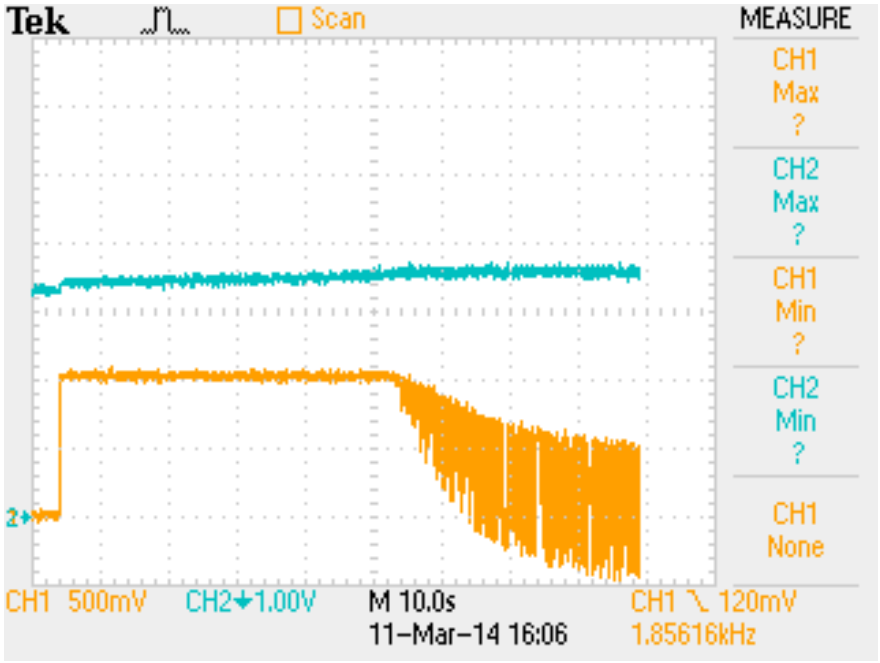

Figure 20: A screenshot of the drain current (CH1) and cell voltage (CH2).

The current was measured by using a 0.1 Ω sense resistor between the cell's positive terminal

and the drain of the MOSFET. Positive voltages represent current flowing into the cell, negative voltages represent currents flowing out of the cell. The sense resistor was removed when the devices were wired to the pack. During test cycles, the circuit was not allowed to run long enough to start drawing current out of the cell.

After the balancing system was confirmed to be functional, a new battery pack was made including the balancing circuits. The voltage curves of the charging phase are shown in Figure 21. The new pack was cycled over 100 times with no balancing issues. There were noise problems on channel 4 which also affected channel 5 when the individual cell voltages were calculated. These results are shown in Figures 22 to 23 on the following page.

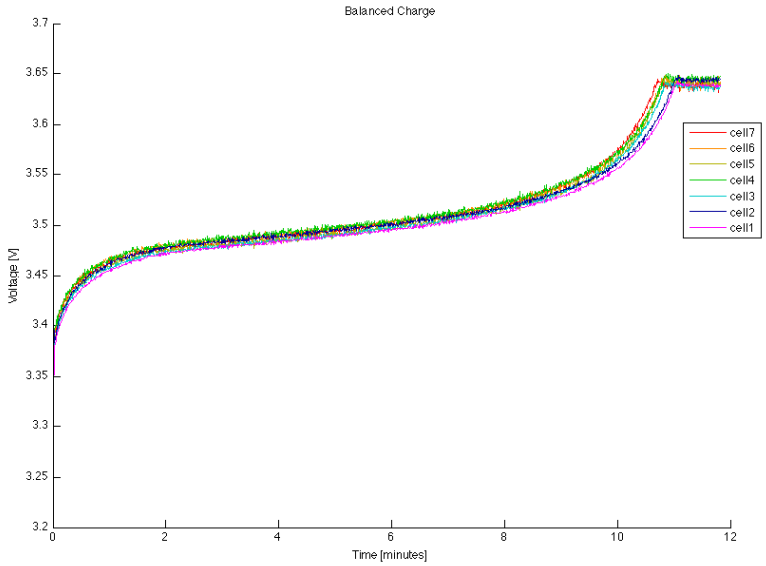

Figure 21: The charging phase with the balancing circuit incorporated.

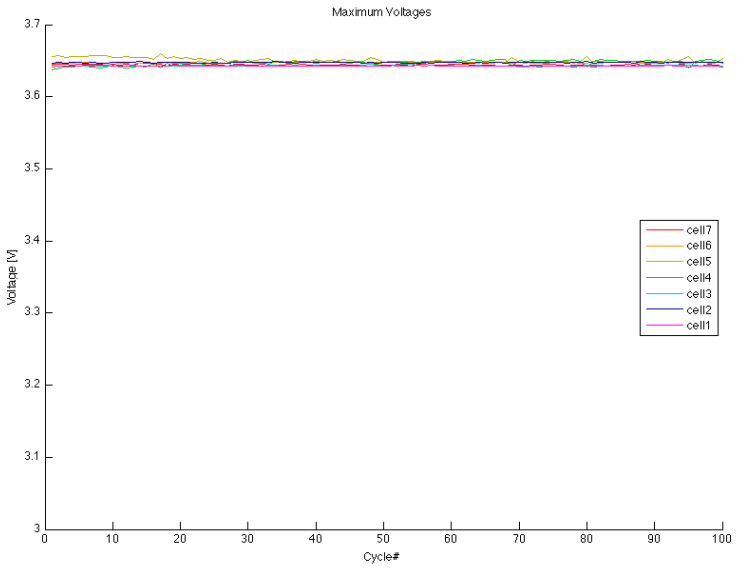

Figure 22: Results of the life test after the balancing circuit was added. This plot shows the maximum voltages during charge.

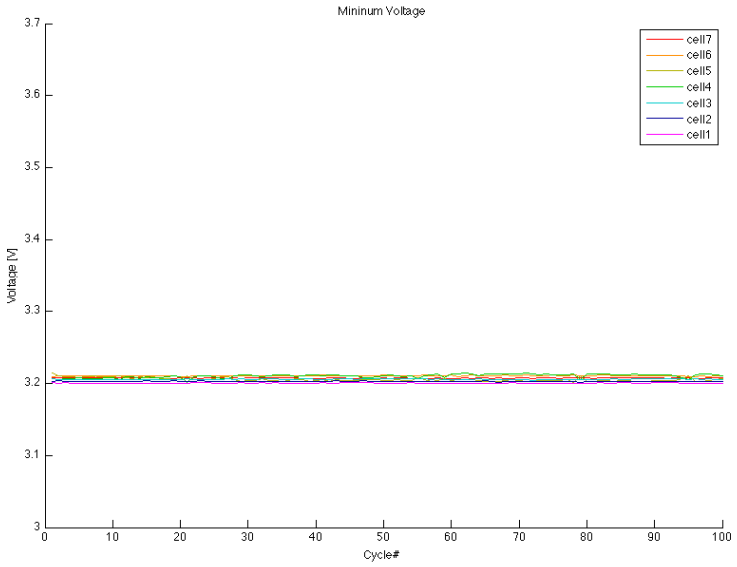

Figure 23: Results of the life test after the balancing circuit was added. This plot shows the minimum voltages during discharge.

6 Conclusions

The 5°C results are very important for underwater charging because, at depth, water temperatures can be as low as 4°C. If the battery pack reaches this temperature in a discharged state, it is

important to heat the pack to a reasonable temperature either by using an external power source or the pack power. We will proceed to investigate weather we can use less than 10% of the energy remaining in the cells to heat them and get an increase of more than 10% in accumulated energy.

Balancing is a know issue with series connected batteries, especially at high charge rates. Section 5.2.5 describes how this problem has been solved. The circuit essentially employs over voltage protection (OVP) and in doing so, all cells in the pack are charged to the same potential. There was no disbalance observed in the discharge phase because the rate was very slow ≈0.25C (0.6A). Comparing figures 17 to 18 on pages 20–21 to Figures 22 to 23 on the previous page, we can see a clear improvement when the circuit is employed.

This project will continue by increasing the power capacity of the battery. We are currently investigating A123 prismatic LiFe-PO_4 cells (AMP20) which have a capacity of 19.6Ah in a single cell. These cells can also be charged at 4C, which means we will be using ≈80A charge current. A 7-cell series connected pack using the prismatic cells will have an energy capacity of ≈440kWh. A new monitoring system to measure voltage and temperature referenced to each cell separately is currently being designed. This will allow for a larger pack to be made because there is no longer a common mode limitation on the analog to digital converter IC.

A Lithium Polymer Comparison

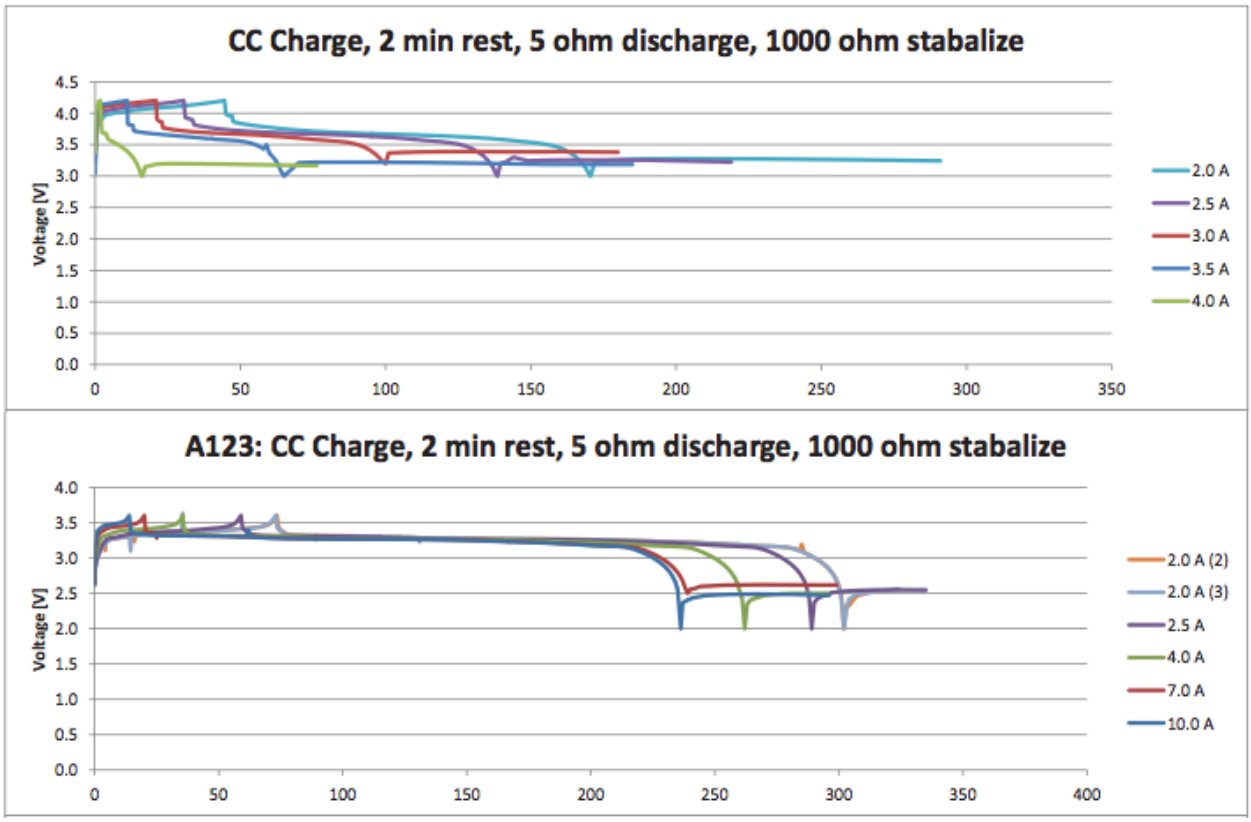

Figure 24: Charging LiPo (top) and LiFe-PO_4 (bottom) at increasing rates

B Data Acquisition Schematics

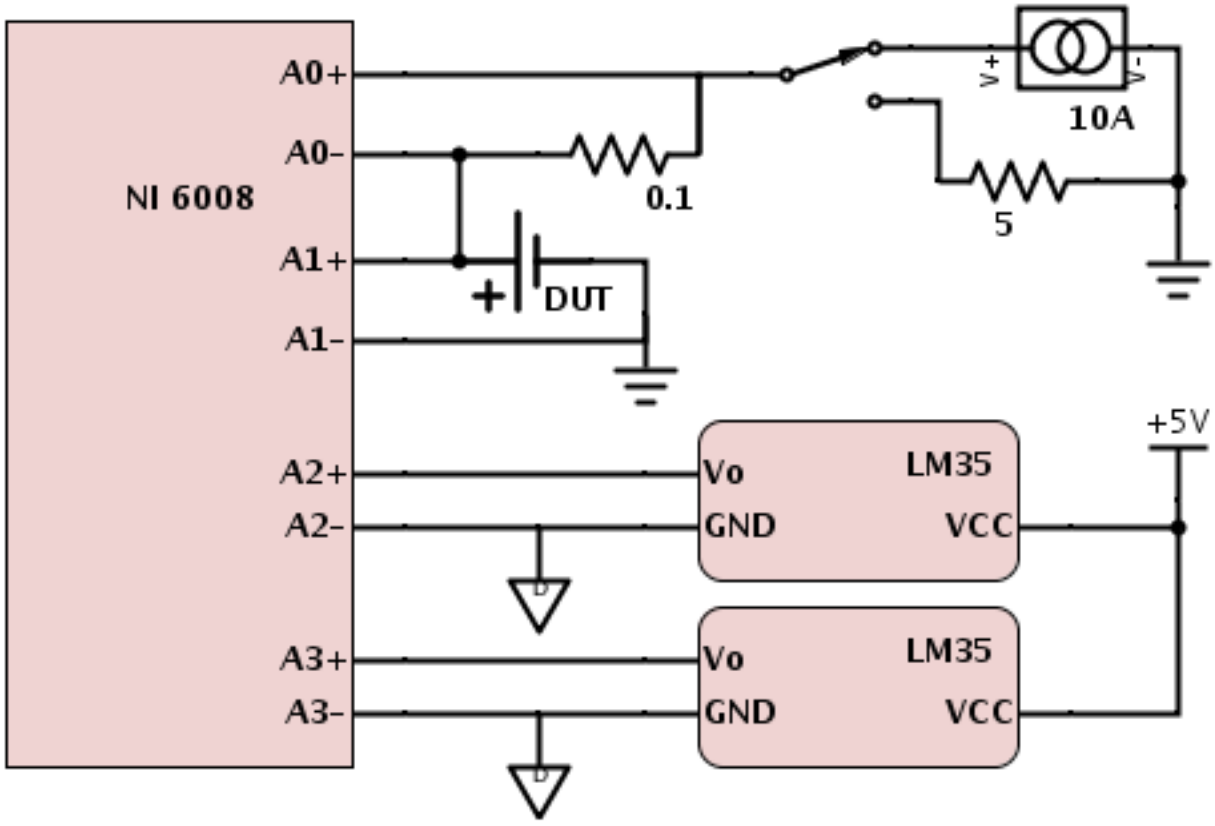

Figure 25: A schematic diagram of the measurement system for the single cell experiments.

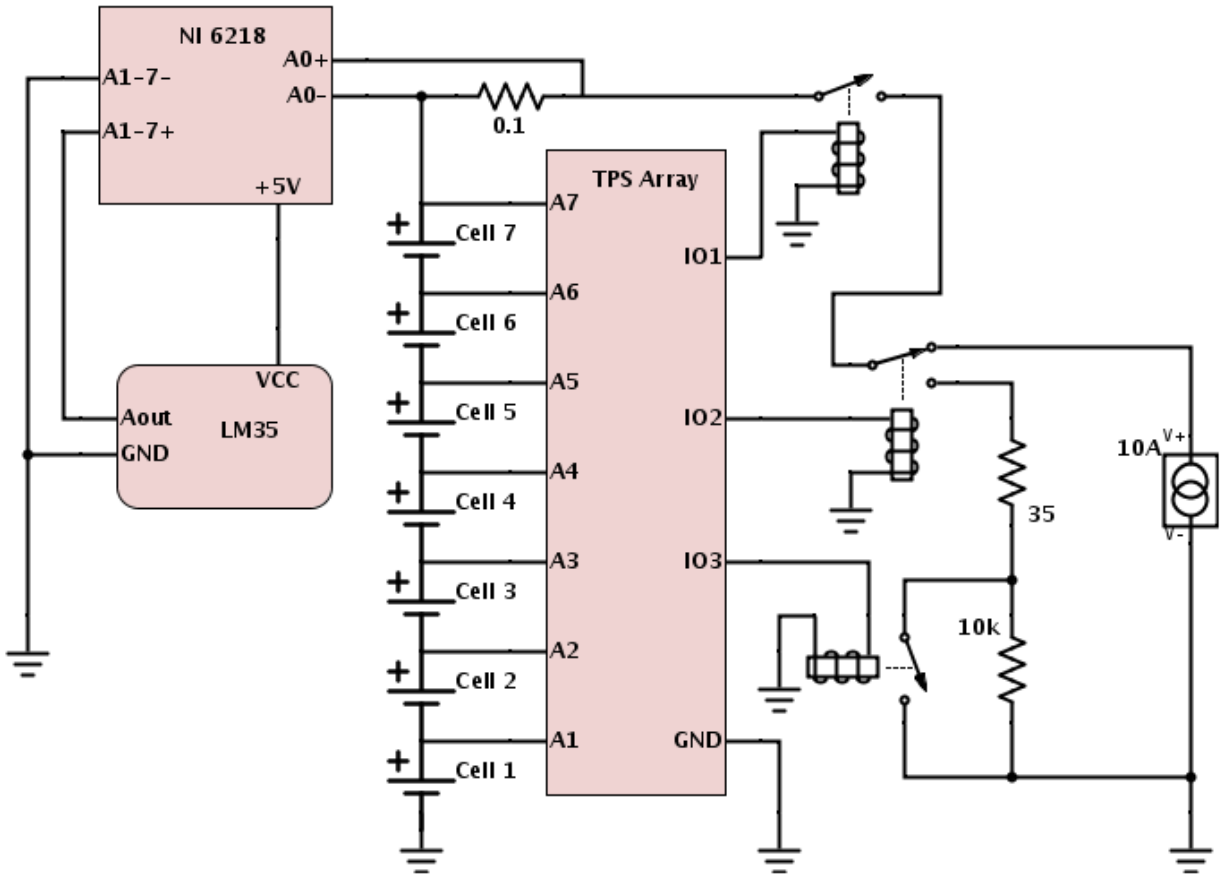

Figure 26: A schematic diagram of the measurement system for the seven cell experiments.

C Oven and Refrigerator Characteristics

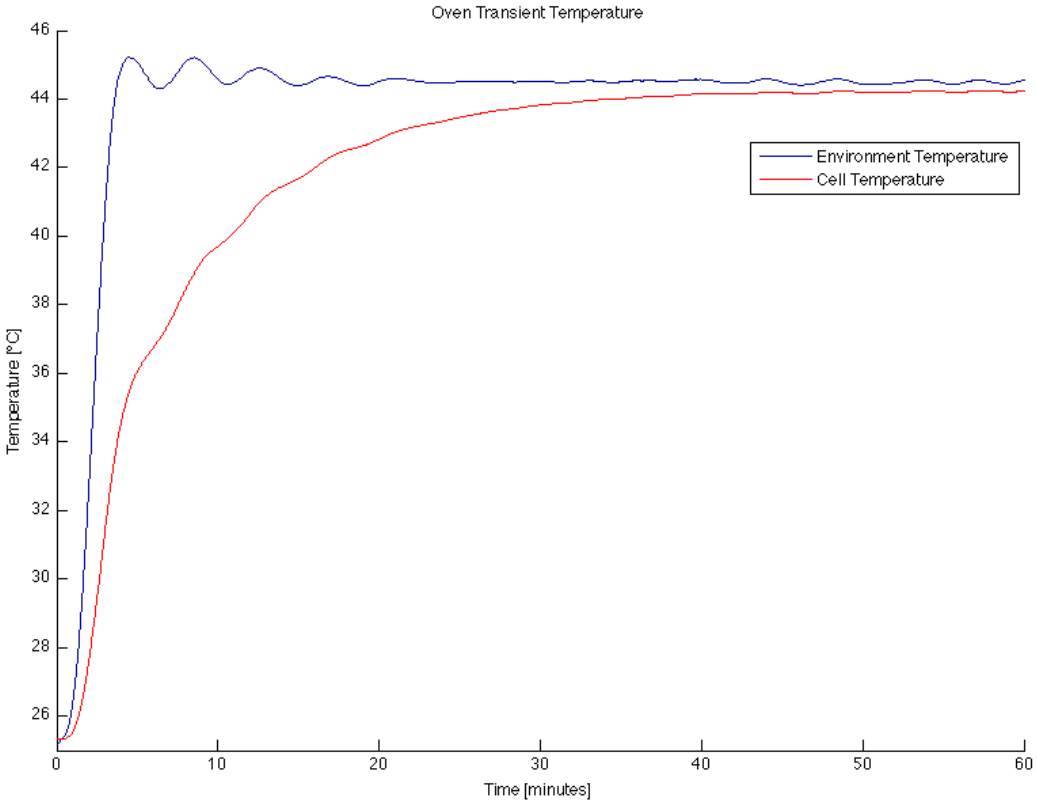

Figure 27: The oven temperature reaches the desired temperature in about 10 minutes, while the cell temperature takes about 1 hour to reach 40°C

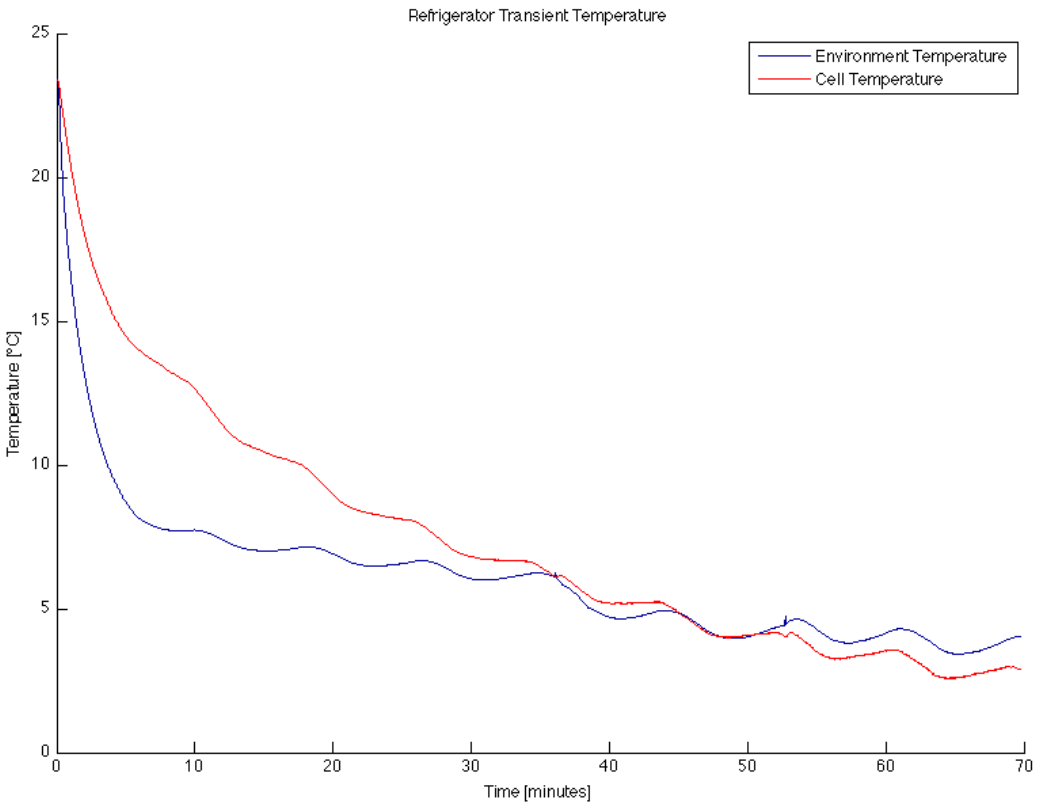

Figure 28: The temperature fluctuations of the refrigerator are due to the compressor turning on and off

D Full data sets

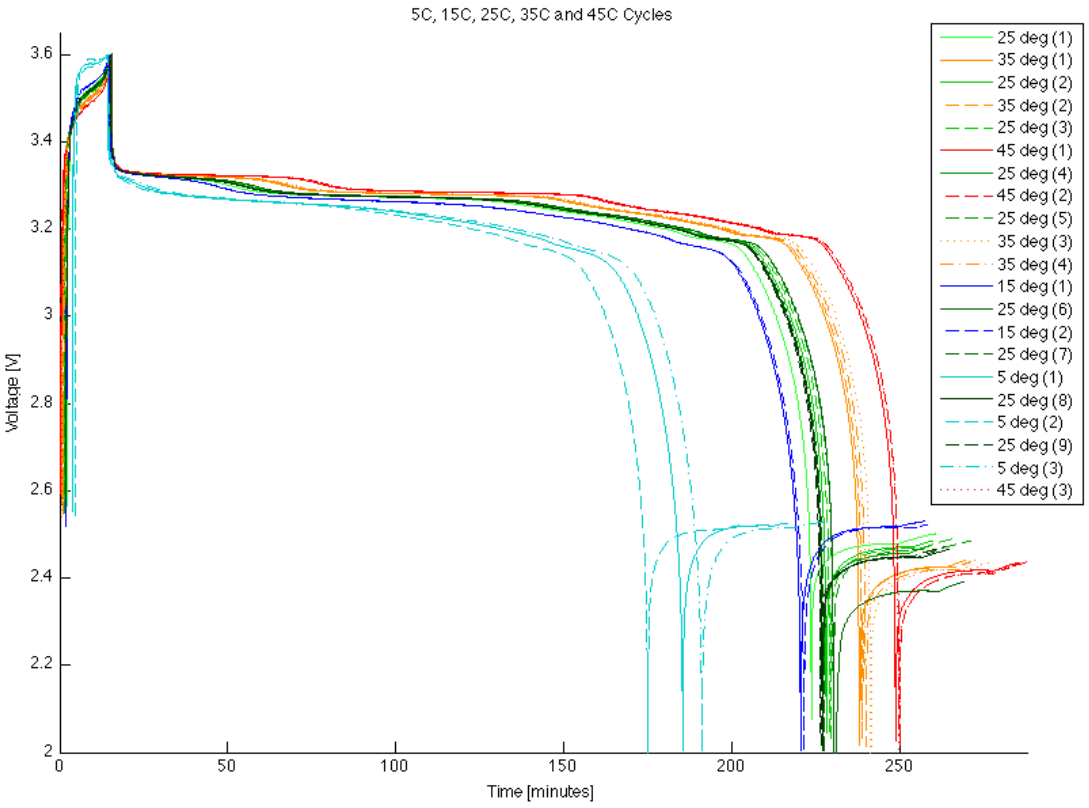

Figure 29: All data recorded for temperature experiments done on a single cell.

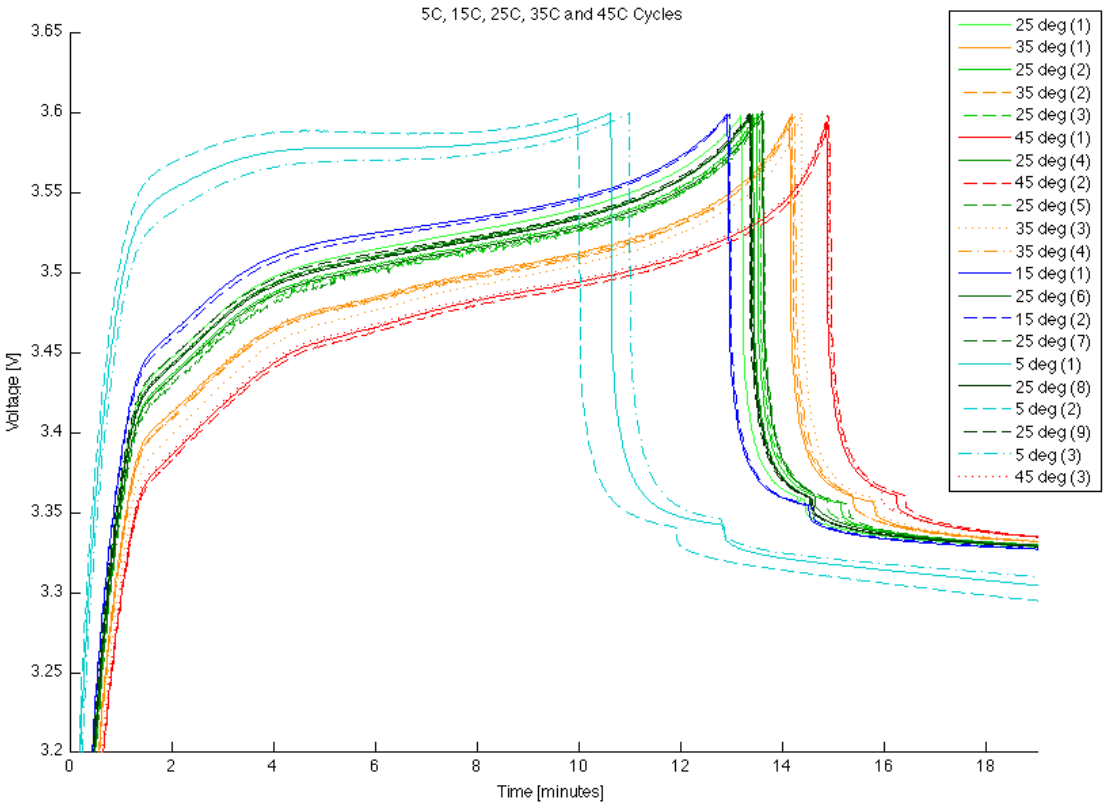

Figure 30: Zoomed view of preceding figure

E Pack Temperature Experiments

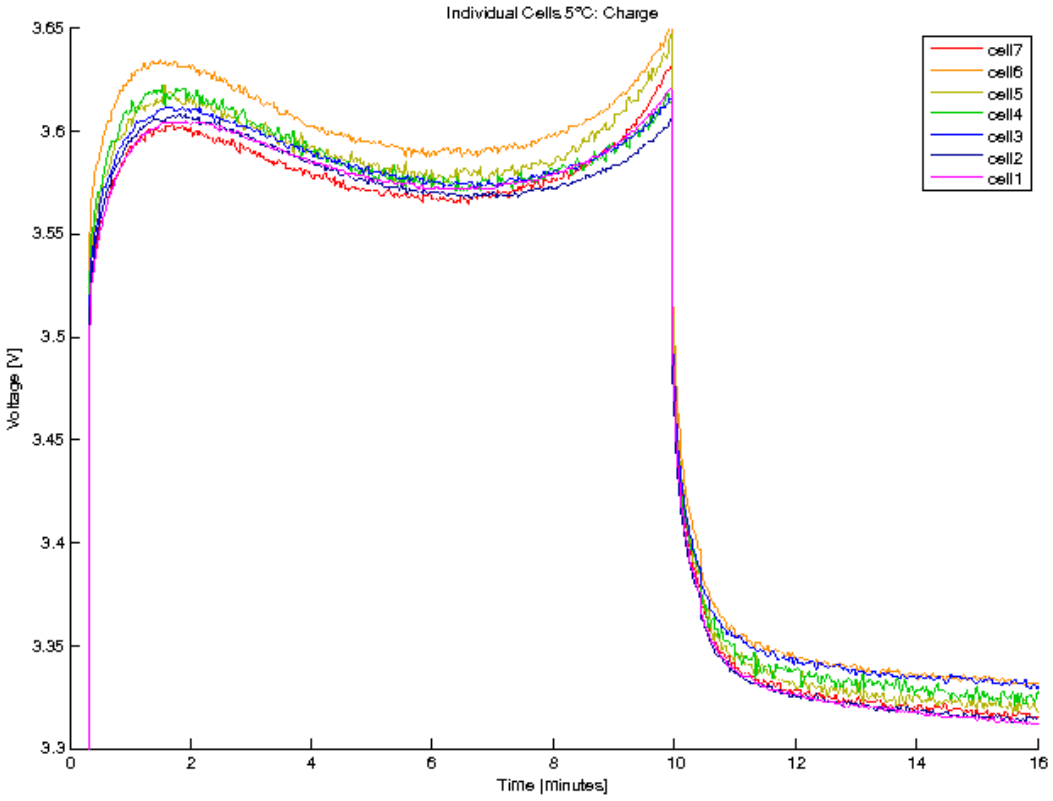

Figure 31: Charge phase of individual cell voltages in a 7-cell pack charged at 5°C

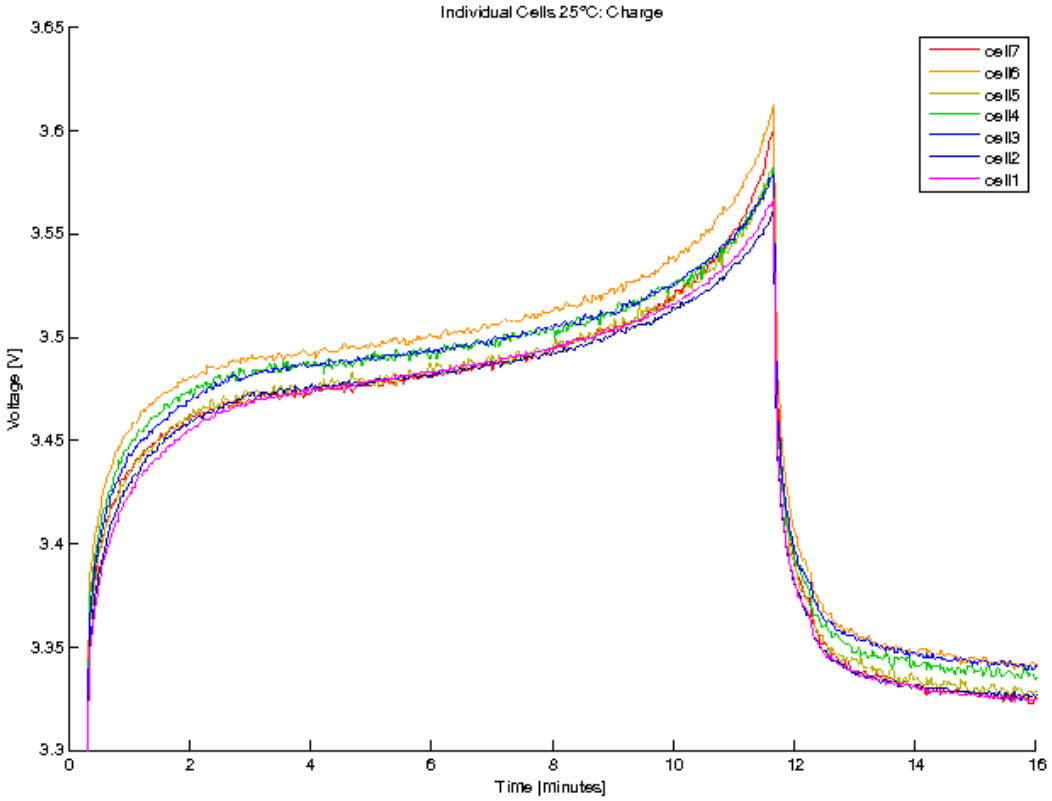

Figure 32: Charge phase of individual cell voltages in a 7-cell pack charged at 25°C

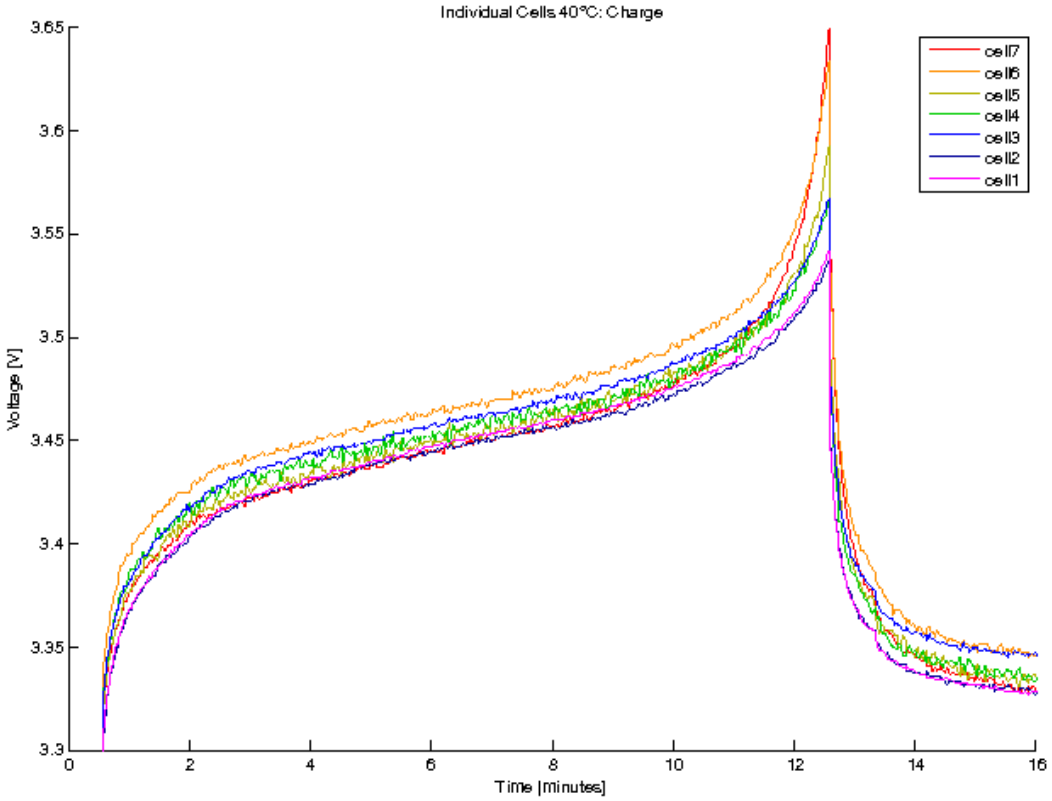

Figure 33: Charge phase of individual cell voltages in a 7-cell pack charged at 40°C

F Charging Algorithms

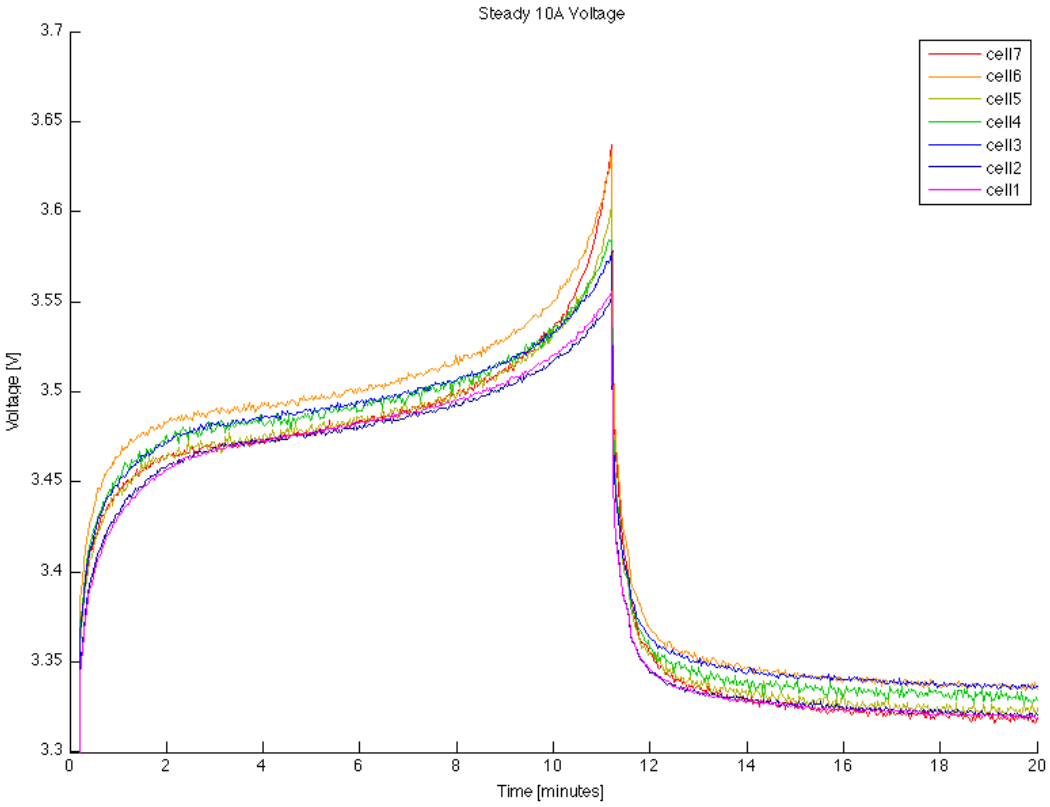

Figure 34: Constant Current charging unbalance.

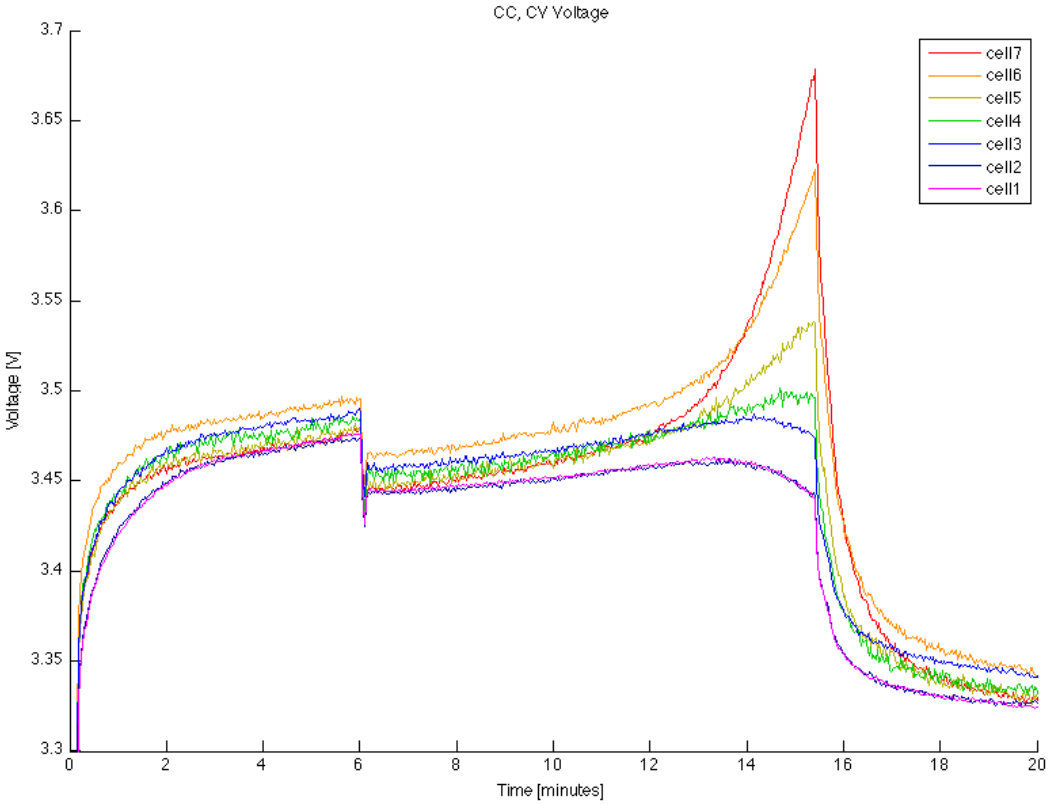

Figure 35: Constant Current/Constant Voltage charging unbalance.

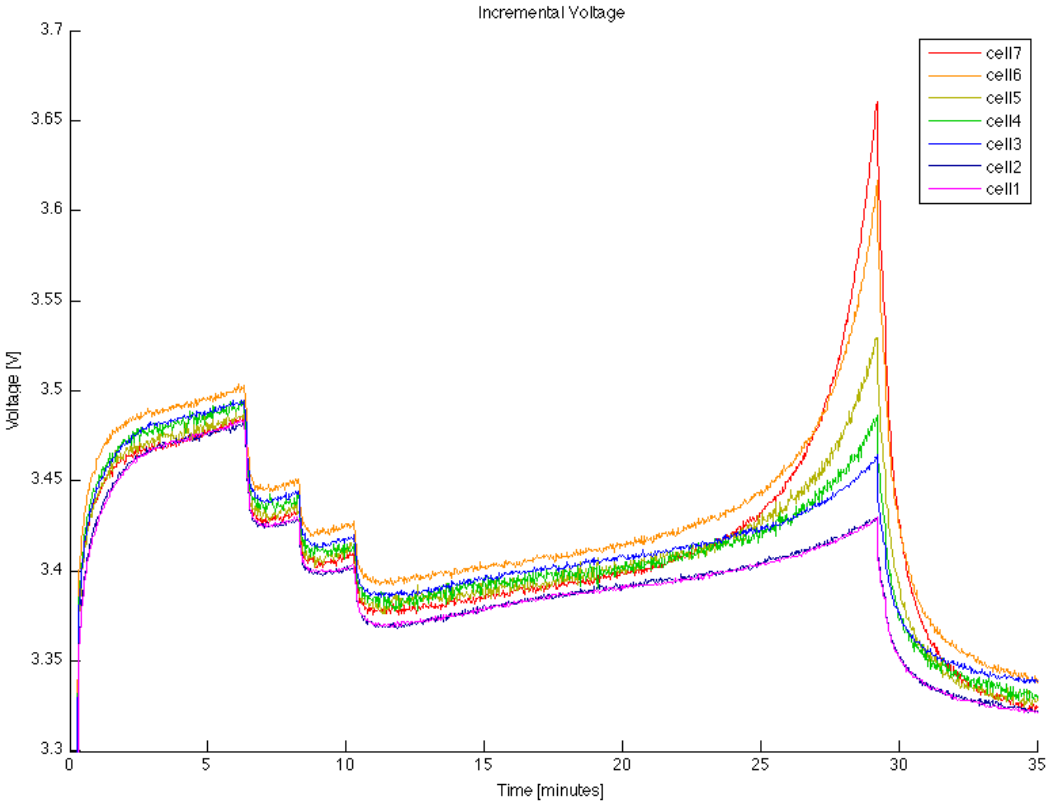

Figure 36: Constant Current charging unbalance.

References

[1] *Nanophosphate High Power Lithium Ion Cell ANR26650M1-B*, A123 Systems, Inc., 2011.

[2] *Positive Voltage Intelligent Protection Device Hotswap Controller and I^2C Current Monitor*, Texas Instruments, April 2010, rev. B.